

Second Order Fading Statistics on WWSUS Channels

Victor M. Hinostroza and Alejandra Mendoza

Abstract. The frequency and time selectivity of the fading channel is an important characteristic for characterization and estimation of such channels. To characterize this type of channels the second order statistics are used. One of the tools used for this characterization is Jake's simulator. This simulator is compared to actual measurements in this work. The second-order statistics level crossing rate (LCR) and average duration of fading (ADF) are two parameters that are reviewed and analyzed here. Analysis of LCR and ADF in several environments was performed. LCR is calculated in several envelope thresholds and its relationship with envelope change is analyzed. Average duration of fades (ADF) for several thresholds is calculated and analyzed. Graphics are provided of LCR and ADF for several different indoor environments. PDF for fading characteristics are derived.

Keywords. Average duration of fades, channel characterization, fading channels, frequency selectivity.

I. INTRODUCTION.

In mobile radio communications the signal envelope suffers from fading. The second order statistics of the fading time intervals are of high importance in the design, development and performance analysis of mobile radio communications systems. The basic idea of all diversity methods is to combine several independent copies of the signal at the receiver. Applications of this concept include the adaptive receivers and the use of multiples antennas. The paths over which the signals propagate are not independent and identically distributed. So, the components of the transmitted signals at the receiver have different fading distributions and are mutually correlated. The level crossing rate is an indication of the fading rate and an important parameter for diversity systems. The level crossing rate (LCR) is a second order statistic of this fading and is affected by the speed of the mobile receiver. Other parameters of interest are the autocorrelation and cross correlation properties of the underlying process. There are several methods based on the Jakes simulator [1] used for simulation of these parameters. Many different techniques [9], [10], [11] has been proposed for the simulation and modeling of mobile radio channels en general and the autocorrelation, cross correlation, LCR and ADF in particular.

Manuscript received September 15, 2007. Revised version received Oct. 6, 2007. This work was supported in part by a grant from the Program PROMEP of the Mexican Government the and a internal grant from the UACJ.

V. Hinostroza and A. Mendoza are with the Electrical and Computation Engineering Department of the University of Ciudad Juarez in Mexico.

However, most of these techniques are analytical and do not have many practical results to confirm the analysis. In this work, comparison of these parameters with actual measurements is presented. In part II a description of the theoretical basis is reminded and a description of the measurement environments is provided. In part III resultant graphs of the analysis are presented along with an explanation of how they were derived. And in the final part conclusions are provided.

II. THE MATHEMATICAL REFERENCE MODEL.

The received signal envelope experiences fades whenever the transmitter or the receiver moves. In addition to that, the surroundings of the communication channel also changes with time, causing fading. Some of the parameters of our interest are to know the average number of times the signal fades below a threshold and the average length of time that the signal stays below it. The signal fade rate may be characterized by the number of times the envelope crosses a threshold level in a unit of time. It is evident that the level crossing rate is directly related to the speed of the receiver since a faster receiver will modify the conditions of the channel more frequently. Several works have attempted to model the crossing rate statistically but in the absence of the second order statistics, modeling should be empirical. [3], [4], [5], [6]. The level crossing rate at envelope R is defined as the rate at which a fading signal envelope crosses level R in any direction. In general, is given by [1] [9]:

$$N_R = \int_0^{\infty} \dot{r} p(R, \dot{r}) d \dot{r} \quad (1)$$

Where the dot indicates the time derivative and

$p(R, \dot{r})$ is the joint probability density function of r and \dot{r} , respectively. Another common definition of N_R is the following:

$$N_R = \sqrt{2\pi} f_m \rho e^{-\rho^2} \quad (2)$$

Where

$$\rho = \frac{R}{R_{RMS}} \quad (3)$$

Here appears the term f_m Doppler frequency, which denotes the LCR dependency on receiver speed.

The average duration of fades is the average length of time for which the signal envelope remains below a threshold of signal level. LCR y ADF may be used to determine the impact of fading on digital transmission systems particularly in packet transmission systems operating in fading mobile radio systems. In these systems, ADF may serve as a guide to the design of packet radio systems.

The average fade duration is defined as the average period of time for which the received signal is below a specified level R. For a Rayleigh fading signal, this is given by:

$$\bar{\tau} = \frac{1}{N_R} \Pr[r \leq R] \tag{4}$$

Where $\Pr[r \leq R]$ is the probability that the received signal r is less than R and is given by:

$$\Pr[r \leq R] = \frac{1}{T} \sum_i \tau_i \tag{5}$$

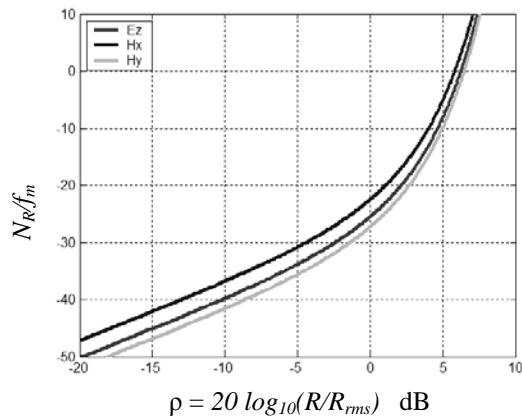


Figure1 Normalized LCR of the three fields components

Where τ_i is the duration of the fade and T is the observation interval of the fading signal. The probability that the received signal r is less than the threshold R is found from the Rayleigh distribution as

$$P_r[r \leq R] = \int_0^R p(r)dr = 1 - e^{-\rho^2} \tag{6}$$

Where $p(r)$ is the pdf of the Rayleigh distribution. Thus, using equations (1), (2) and (4), the average fade duration as a function of ρ and f_m can be expressed as

$$\bar{\tau} = \frac{e^{\rho^2} - 1}{\rho f_m \sqrt{2\pi}} \tag{7}$$

Using (1) and (2) and substituting the appropriate values of the moments, we get the expression of the level crossing rate for the three field components:

$$\begin{aligned} E_Z \quad N_R &= \sqrt{2\pi} f_m \rho e^{-\rho^2} \\ H_X \quad N_R &= \sqrt{\pi} f_m \rho e^{-\rho^2} \\ H_Y \quad N_R &= \sqrt{3\pi} f_m \rho e^{-\rho^2} \end{aligned} \tag{8}$$

These three expressions are plotted in figure 1.

Using (7) we can obtain also, the three expressions for the average duration of fading, then we get.

$$\begin{aligned} E_Z \quad \bar{\tau} &= \frac{e^{\rho^2} - 1}{\rho f_m \sqrt{\pi}} \\ H_X \quad \bar{\tau} &= \frac{e^{\rho^2} - 1}{\rho f_m \sqrt{2\pi}} \\ H_Y \quad \bar{\tau} &= \frac{e^{\rho^2} - 1}{\rho f_m \sqrt{3\pi}} \end{aligned} \tag{9}$$

These three expressions are plotted in figure 2.

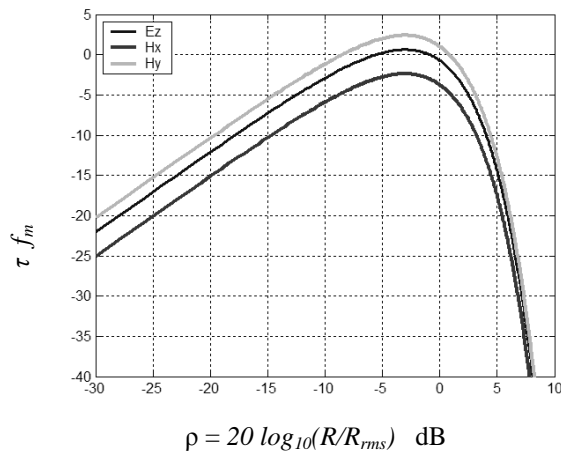


Figure 2 Normalized ADF of the three fields components.

A reference model for the received complex low pass envelope is a complex Gaussian noise process

$$\mu(t) = \mu_1(t) + j\mu_2(t) \tag{10}$$

Where $\mu_1(t)$ and $\mu_2(t)$ are uncorrelated zero-mean real Gaussian noise processes with identical variances $\sigma_0^2 = E\{\mu_i^2(t)\}$ ($i = 1, 2$). Then the autocorrelation function (ACF) of the stochastic process $\mu(t)$ and $\mu_i(t)$, are given by

$$\begin{aligned} r_{\mu\mu}(\tau) &= 2\sigma_0^2 J_0(2\pi f_{\max} \tau) \\ r_{\mu_i\mu_i}(\tau) &= \sigma_0^2 J_0(2\pi f_{\max} \tau), \quad i = 1, 2 \end{aligned} \tag{11}$$

Respectively, where $J_0(\cdot)$ is the zero-order Bessel function of the first kind, and f_{max} is the maximum Doppler frequency. In Jakes' simulator the received complex low pass envelope is modeled by:

$$\tilde{\mu}(t) = \tilde{\mu}_1(t) + j\tilde{\mu}_2(t) \tag{12}$$

Where

$$\mu_i(t) = \sum_{n=1}^N c_{i,n} \cos(2\pi f_{i,n} t + \theta_{i,n}), \quad i = 1,2 \tag{13}$$

Represents a superposition of N weighted low frequency oscillators. The deterministic behavior of $\tilde{\mu}_1(t)$ and $\tilde{\mu}_2(t)$ enable us to investigate the correlation properties of these functions by computing the following time average.

$$\tilde{r}_{\mu_i \mu_j}(\tau) = \langle \tilde{\mu}_i(t) \cdot \tilde{\mu}_j(t + \tau) \rangle \tag{14}$$

For all combinations $i,j = 1, 2$, substituting (13) into (14) gives the following analytical expressions

$$\begin{aligned} \tilde{r}_{\mu_i \mu_i}(\tau) &= \sum_{n=1}^N \frac{c_{i,n}^2}{2} \cos(2\pi f_{i,n} \tau), \quad i = 1,2, \\ \tilde{r}_{\mu_1 \mu_2}(\tau) &= \tilde{r}_{\mu_2 \mu_1}(\tau) = \sum_{n=1}^N \frac{c_{1,n} c_{2,n}}{2} \cos(2\pi f_{1,n} \tau) \end{aligned} \tag{15}$$

Let $N \rightarrow \infty$, then substituting (13) in (15) gives

Based on the previous theory, analysis and of the envelope autocorrelation, the envelope cross-correlation, LCR and ADF has been performed on data that was collected in several measurements campaigns. The sounder system used to make the measurements of this work was developed at UMIST in Manchester UK and is described in [2]. This sounder uses the FMCW or chirp technique. The generated chirp consists of a linearly frequency modulated signal with a bandwidth of 300 MHz and a carrier frequency of 2.35 GHz. The bandwidth was from 1960 to 2260 MHz. The chirp repetition frequency is 100 Hertz, which allows having measurements of 50-Hertz Doppler range.

$$\begin{aligned} \lim_{N \rightarrow \infty} \tilde{r}_{\mu_i \mu_i}(\tau) &= \frac{2\sigma_0^2}{\pi} \int_0^{\pi/2} [1 - \cos(4z)] \cos(2\pi f_{max} \tau \cos z) dz \\ &= \sigma_0^2 [J_0(2\pi f_{max} \tau) - J_4(2\pi f_{max} \tau)] \end{aligned} \tag{16}$$

And

$$\begin{aligned} \lim_{N \rightarrow \infty} \tilde{r}_{\mu_2 \mu_2}(\tau) &= \frac{2\sigma_0^2}{\pi} \int_0^{\pi/2} [1 + \cos(4z)] \cos(2\pi f_{max} \tau \cos z) dz \\ &= \sigma_0^2 [J_0(2\pi f_{max} \tau) + J_4(2\pi f_{max} \tau)] \end{aligned} \tag{17}$$

The three environments where the measurements took place were the following: 1) A computer cluster, a three-room computer facility. 2) Around a floor inside a building. 3) Between floors measurements in an eight stories building, measurements were taken at similar locations in different floors. Each location in each environment was sampled during one second and 100 impulse responses were stored for each location.

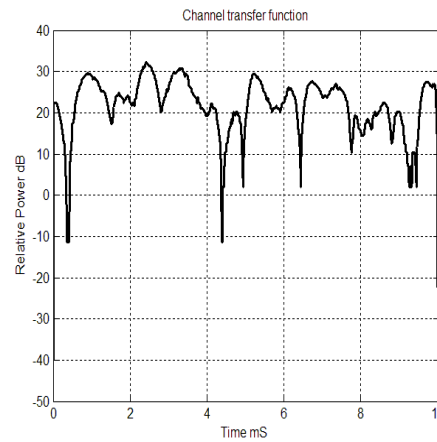


Figure 3. Typical channel transfer function

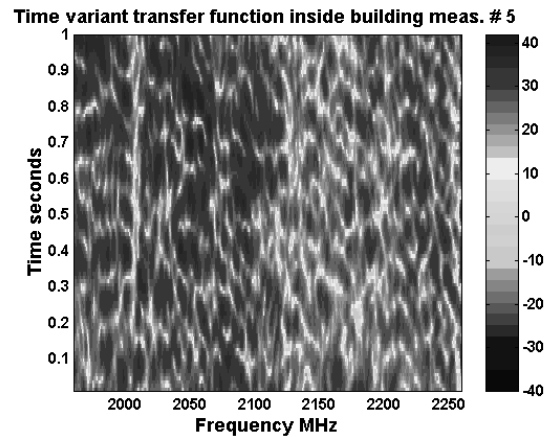


Figure 4. Time variant channel transfer function

The procedure used to make the study was the following: First a channel transfer function for each impulse response was calculated, as is shown in figure 3. This gives us 100 sets of data for each location, for each transfer function the maximum value was calculated. Second, every crossing in the transfer function was recorded, to calculate the crossing a threshold was set, in each environment five different threshold were used; 10, 15, 20, 25 and 30 dB below from the maximum value in the transfer function. As

can be seen in figure 4 the variations on the 100 transfer functions are not important, with this we can use averages instead of using each transfer function. The use of thresholds instead of using RMS envelope values was with the intention of knowing how the fades deep was changing and how deep the fade was. Third, on each location the average of crossings for the 100 sets of data were calculated in each location. This averaging was performed because the time variant transfer function for the sampled time (one second) has no significant deviation. So the averaging reduces the amount of data considerably. Fourth, graphs were done to show the results of the process.

III. LEVEL CROSSING RATE AND AVERAGE DURATION OF FADING

Figure 5 shows the LCR for one of the environments described. Figure 4 shows the LCR for the floor penetration environment. In this environment the location number indicates the number of floors the signal has to penetrate, that because the higher the number of the location, the higher the number of crossings at all thresholds. In this environment the fades were deep and lengthy; this is observed when in the different thresholds the number of crossings stays more or less in the same value. In this environment, the number of crossings is relatively high, this could be because of the signal has to travel through the windows and follow paths outside the propagation indoor channel and the number of scatterers that participate in the multi-path signal is higher.

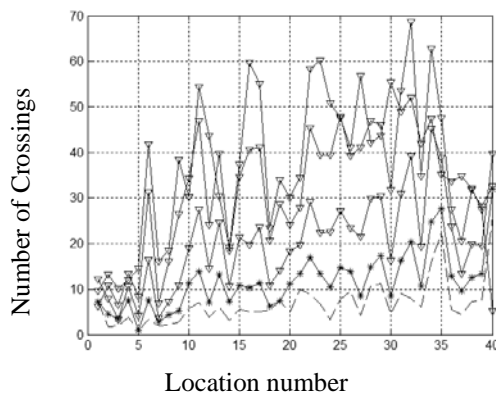


Figure 5. LCR for floor penetration

Figure 6 shows for the floor penetration environment. In this figure it is possible to see that the average for the 10 dB threshold is about 4.5 milliseconds higher than the other environments discussed. The difference between the average of the 10 dB and the 20 and 30 dB thresholds is of about 3 milliseconds, also higher than the other environments. Moreover, in the 10 dB threshold there is a tendency of the ADF to increase as the number of location increases, that is to say, as the number of floors the signal has to penetrate increases, the fading increases. The ADF for the 30

dB threshold is almost non existent; most of the locations have an ADF of less of 0.5 milliseconds for this threshold.

Figures 7, 8 and 9 show a comparison of the autocorrelation and cross correlation functions of an analytical waveform and an actual measurement. In order to generate the function for the analytical autocorrelation, the delay spread is assumed to have an exponential decay. But when we used the data generated by the measurement this condition is not present in most of the measurements. So, when we try to generate the Bessel function with real data, produces not usable graphs. What we have to do was to sort the delay data from zero to maximum delay and then generate the graph. Even though the real delay is not in order it represent the actual maximum delay and a comparison can be made.

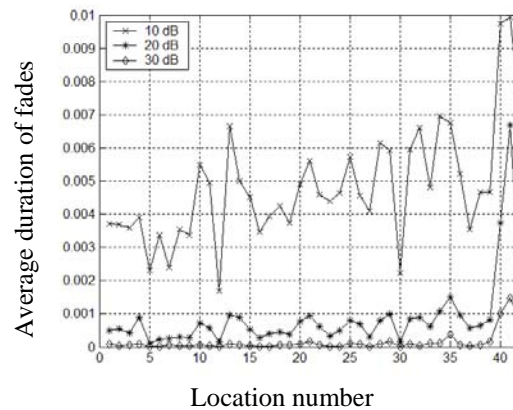


Figure 6. ADF for floor penetration.

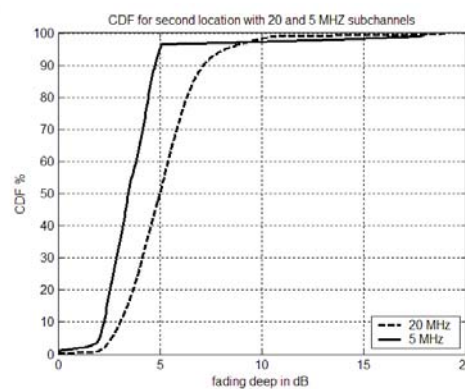


Figure 7 Fading CDF for building to building

A different way to look at the statistics of the fading is to calculate the CDF of this parameter. To make the calculations of these CDF's figures, the mean of all locations in the involved environment were used. Figure 7 shows the CD of the building-to-building environment for both, the 20 and 5 MHz bandwidths, this figure shows that the fading deep for a 20 MHz sub channel is below 7 dB for 90% of the times. On the other hand, for the 5 MHz sub channel, the fades are below 5 dB for 90% of the times. Figure 8 shows

the CDF's for the large laboratory environment; here both sub channels bandwidths; 5 and 20 MHz, are below 5 dB most of the times. Even though, the 5 MHz sub channel is below 3 dB for 90% of the times.

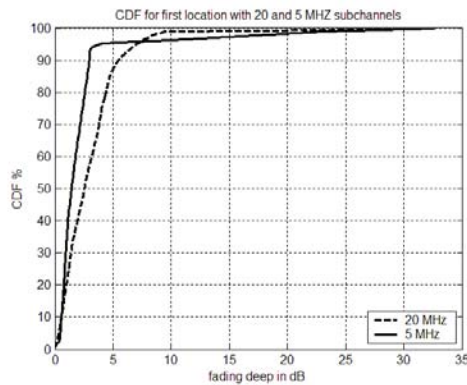


Figure 8. Fading CDF for large laboratory

IV. AUTO AND CROSS CORRELATION ENVELOPE FUNCTIONS.

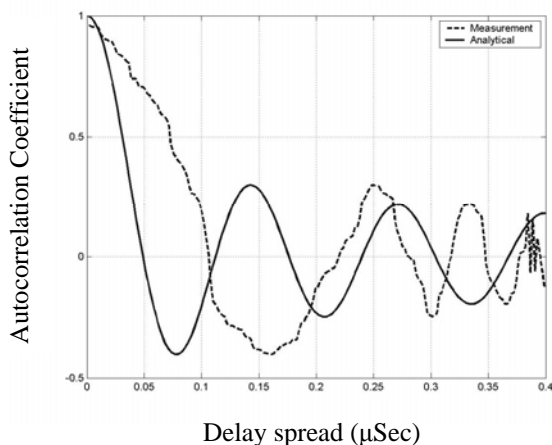


Figure 9. Comparison of correlation coefficient.

Figures 9, 10 and 11 were generated using expressions (16) and (17). Figure 9 shows the autocorrelation function for the two sets of data. This figure shows that even when the shapes of the correlations are consistent, they do not have the same signature. Real data takes more time to reach the first crossing by zero correlation and this happens in the other figures too. And the peaks and valleys are out of phase most of the time. Figure 10 shows the power of two of the autocorrelation function, here again is possible to see that the decay time of the correlation coefficient value is higher for the analytical than for the measurement data and the asymptotic decay to zero is faster in the real data. Figure 11 shows the cross correlation functions of the same data. In this case the swing of the value of correlation is higher than the autocorrelation and again the peaks and valleys are out of phase.

V. CONCLUSIONS.

Analysis of correlation, LCR and ADF of practical measurements has been presented. From the results, it is possible to conclude that each environment presents different behavior about LCR. Even in similar open spaces such as the floor penetration and inside building, the behavior is quite different, as can be seen in the preceding figures.

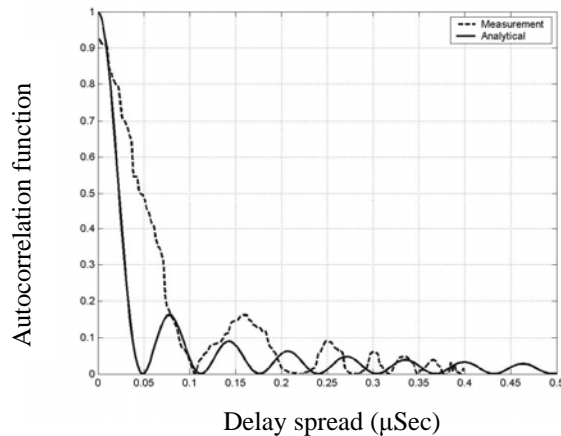


Figure 10. Comparison of correlation coefficient.

Regarding LCR of the four environments studied three of them, have less than 30 crossings at the minimum threshold 10 dB. The other environment; floor penetration, show a number of crossings higher than 50, this environment have the larger delay spread. On the other hand, in all environments, the minimum threshold of 30 dB, have less than 10 crossings in all locations.

Regarding ADF results shows that similar environments, i.e.; floor penetration and inside building have similar ADF behavior, even when other parameters, like LCR and delay spread, are different. The ADF for the floor penetration environment shows some high values compared to the other two environments, but most of the values are within the values observed.

Analyzing all the environments together, the ADF for the maximum threshold 10 dB is most of the time below 7 milliseconds and for the minimum threshold 30 dB, is always less than 1 millisecond. Which confirms that deep fades are rare and of short duration.

Still is possible to get more information from these measurements. The possible analyses that can be done are the following parameters; the relationship of delay spread and number of fades, the fade movement in the sampled period, study of the relationship of LCR with the SNR of the signal, CDF and PDF of the fading rate and the fade deep related to the fade location in time.

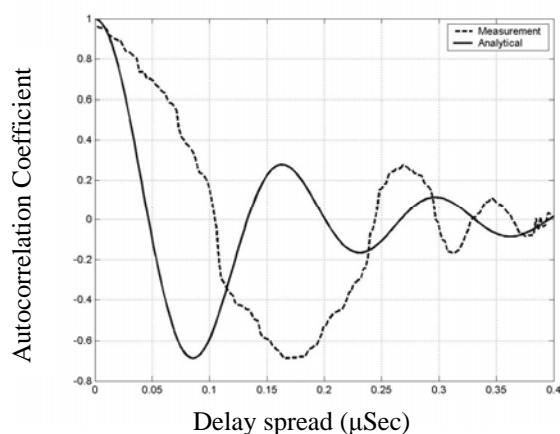


Figure 11. Comparison of correlation coefficient.

In the correlation revision it was found that all real data takes more delay time than simulated data to reach the same correlation coefficient values and the decay to zero is faster. Now, the error between the real and simulated data will also depend on how many signals are taking into account in the simulation. Other parameter that could be used is to calculate the cross correlation between clusters or components of the power delay profile. And it will be necessary to test the “ergodicity” of the real and simulated data.

References.

1. Jakes W. C., *Microwave Mobile Communications*, John Wiley and sons, 1974.
2. Salous S, Hinostroza V, "Bi-dynamic indoor measurements with high resolution sounder", 5th. International Symposium on wireless multimedia Communications, Honolulu Hawaii USA, October 2002.
3. Beaulieu N. and Dong X., "Level crossing rate and average fade duration of MRC and EGC diversity in Rician Fading", IEEE transactions in communications, Vol. 51, No. 5, May 2003, pp. 722-726.
4. Xiao C. and Zheng Y., "A generalized simulation model for Rayleigh fading models with accurate second-order statistics", VTC 2002, pp. 170-174.
5. Chacraborty S. and Yong L., "Level crossing rate and average fade duration of the select and hold policy of selection diversity combining in Rayleigh fading channel", IEEE communications letters, Vol. 8, No. 6, June 2004, pp. 371-373.
6. Patzold M., Youssef N. and Wang C., "Level crossing rate and average fade duration of deterministic simulation models for Nakagami-Hoyt fading channels", The 5th. Symposium on wireless personal multimedia communications, Vol. 1, October 2002, pp. 272-276.
7. Kaveh M. and Abdi A., "Level crossing rate in terms of the characteristic function: A new approach for calculating the fading rate in diversity systems.", IEEE transactions on communications, Vol. 50, No. 9, September 2002, pp. 1397-1400.
8. Patzold M. and Laue F., "Statistical Properties of Jakes' Fading Simulator", in Proc. IEEE VTC Spring, May 1998, pp. 712-718.
9. Yoo D. and Stark W., "Characterization of WSSUS Channels: Normalized Mean Square Covariance", IEEE Trans. On Wireless Communications, Vol. 4, July 2005, pp. 1575-1584.
10. Lee W. C. Y., *Mobile Communication Engineering*, (McGraw-Hill, 1998)
11. Bello P.A., "Characterization of randomly time-variant linear channels", *IEEE Transactions on Communications Systems*, December 1963, pp. 360-393.
12. Bultitude R., "Measurement Characterization and Modelling of Indoor 800/900 MHz Radio Channels for Digital Communications", *IEEE Communication Magazine*, June 1987, Vol.25, No.6, pp. 5-12.
13. Clarke R.H., "A statistical theory of mobile radio reception", *Bell Systems Technology Journal*, Vol. 47, pp. 957-1000
14. Salous S., and Hinostroza V., "Bi-dynamic UHF channel sounder for Indoor environments", *IEE ICAP 2001*, pp. 583-587.